

Determination of Spatiotemporal Structure of Fluctuations by Statistical Averaging Method^{*)}

Yuichi KAWACHI, Sigeru INAGAKI^{1,2)}, Kentaro TOMITA, Kotaro YAMASAKI¹⁾, Fumiyoshi KIN, Yusuke KOSUGA^{1,2)}, Makoto SASAKI^{1,2)}, Yoshihiko NAGASHIMA^{1,2)}, Naohiro KASUYA^{1,2)}, Kazunobu HASAMADA, Boyu ZHANG and Akihide FUJISAWA^{1,2)}

*Interdisciplinary Graduate School of Engineering Sciences, Kyushu University,
6-1 Kasuga-koen, Kasuga 816-8580, Japan*

¹⁾Research Center for Plasma Turbulence, Kyushu University, 6-1 Kasuga-koen, Kasuga 816-8580, Japan

²⁾Research Institution for Applied Mechanics, Kyushu University, 6-1 Kasuga-koen, Kasuga 816-8580, Japan

(Received 29 January 2018 / Accepted 23 July 2018)

Spatiotemporal structure of fluctuation with 11 kHz excited in a linear magnetized plasma was observed in details by applying pattern recognition method based on statistical averaging. Statistical behaviors of instantaneous period of the fluctuation and the temporal behavior of the radial profile of the fluctuation are clarified. Two-dimensional structure of the fluctuation is reconstructed and distortion of the wave-front of the fluctuation was inferred.

© 2018 The Japan Society of Plasma Science and Nuclear Fusion Research

Keywords: non-linear wave, plasma turbulence, conditional averaging, phase tracking, spatiotemporal structure

DOI: 10.1585/pfr.13.3401105

1. Introduction

Pattern recognition becomes important recently and is used to detect anomaly and to reduce dimensionality in a broad range of fields, e.g. imaging science and weather forecasting. An identification of spatiotemporal patterns of fluctuating structures in magnetized plasma is an important task for plasma turbulence research. When the fluctuation amplitude becomes large, the linear approximation breaks down. While linear theory predicts exponential growth of unstable fluctuations, but nonlinear effects cause saturation and limit the fluctuation amplitude at a finite level. In addition, nonlinear processes can distort waveform of waves as observed in ultrasonic waves and shock waves. In fact, density fluctuation in a linear magnetized plasma saturates and its normalized level reaches up to 30 % [1]. Hence nonlinear effects must be taken into account. Spatiotemporal pattern is an important information to identify instabilities and nonlinear interactions in plasma turbulence [2–4]. The waveform distortion of drift waves in magnetized plasma is related to nonlinear processes through wave-front twisting, e.g. formation of the zonal flow and streamer [2,5]. Here we described a method to extract the distorted waveform from turbulent fluctuation signals measured in a laboratory magnetized plasma for understanding nonlinear mechanisms in plasma turbulence.

2. Experimental Setup and Conditional Averaging

We investigate plasma turbulence in a laboratory magnetized plasma. Turbulence is excited in a linear magnetized plasma device, PANTA [6]. Argon plasma is produced by helicon wave ($P_{rf} = 6$ kW, 7 MHz) and injected neutral argon pressure is 3 mTorr. The length of cylindrical plasma is 4 m and diameter of quartz tube of the helicon source (= 100 mm) determines diameter of plasma of approximately 120 mm. Axial magnetic field is $B_{ax} = 0.15$ T. Central electron density and temperature are $1 \times 10^{19} \text{ m}^{-3}$ and 3 eV. Under this condition, the 11 kHz fluctuation and its higher harmonics are strongly excited as shown in Fig. 1. Characteristic frequency of fluctuations excited under the standard condition ($P_{rf} = 3$ kW, $B_{ax} = 0.09$ T) is 4–6 kHz. Azimuthal mode number (m) of the 11 kHz fluctuation is found to be $m = 4$ from an azimuthal probe array measurement [5]. Radial profile of ion saturation current is measured with a 5-channel radial probe array ($r = 23, 33, 43, 53, \text{ and } 63$ mm). The azimuthal array and radial array are installed at 1875 mm and 1375 mm in the axial direction from helicon source, respectively. Electron diamagnetic drift velocity v^* and drift frequency f^* are calculated to be $v^* = c_s \rho_s / L_n = 7.0 \times 10^2 \text{ m/s}$ and $f^* = v^* k_\theta / 2\pi = 11.5 \text{ kHz}$, respectively, where c_s is ion sound speed, ρ_s is gyro-radius evaluated by the ion sound speed, $k_\theta = m/r = 100 \text{ rad/m}$, density gradient scale length $L_n = (\nabla n/n)^{-1} = 2.8 \times 10^{-2} \text{ m}$, which is evaluated by radial profile of ion saturation current. The observed frequency of 11 kHz is close to f^* .

author's e-mail: kawachi@riam.kyushu-u.ac.jp

^{*)} This article is based on the presentation at the 26th International Toki Conference (ITC26).

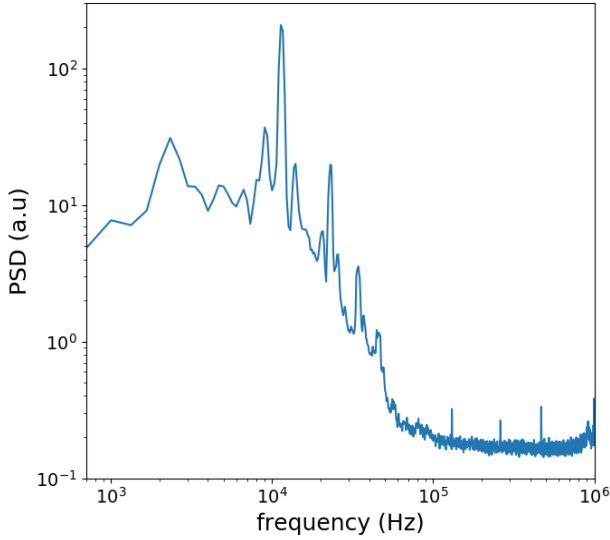


Fig. 1 Power spectrum density (PSD) of ion saturation current fluctuation at $r = 44$ mm.

Here we neglected Doppler shift due to $\mathbf{E} \times \mathbf{B}$ rotation. The background radial electric field of -1 V/cm can explain observed azimuthal velocity. Unfortunately, errors in evaluation of the radial electric field is large due to large level of potential fluctuation ($e\tilde{V}_f/T_e \sim 15\%$) and thus contribution of the background $\mathbf{E} \times \mathbf{B}$ velocity has not been verified yet. On the other hands experimental observation also indicates that levels of normalized density and potential fluctuations are almost the same at $f \sim 11$ kHz. We hence inferred from these that the observed mode is the drift wave.

There are many analysis techniques for quasi-periodical time series data and they are frequently used in plasma turbulence study to analyze pulse-like signals, e.g. blobs and ELMs [7]. Pulse is one of the most obvious signal patterns and thus it is easy to recognize pulses. When there is no apparent pattern in signals, classification of signal based on amplitude is difficult. We thus apply a new method to extract a pattern in signals. This method is based on a technique, which is widely used for heart-beat fluctuation diagnostic by using electrocardiogram [8, 9]. Temporal evolution of ion saturation current at $r = 43$ mm is shown in Fig. 2(a). We are interested in a fluctuating structure with time-length of $100 \mu\text{s}$, which corresponds to high frequency components (≥ 10 kHz) of fluctuation. First, we need initial template to apply our method. The initial template is determined by $f_0(\tau) = \frac{1}{n} \sum_{i=0}^n F(\tau + iT)$ ($0 \leq \tau \leq T$), here $F(t)$ is original signal and characteristic period T is set up by time-scale of interest. In this paper, $f_0(\tau) = \sin(2\pi\tau/T)$ was used for simplicity and T is determined by frequency of the largest peak in ensemble averaged Fourier spectrum. Then we obtained an initial “template” waveform. Next, we calculate cross-correlation coefficient between the template and original signal, $C_j(t)$,

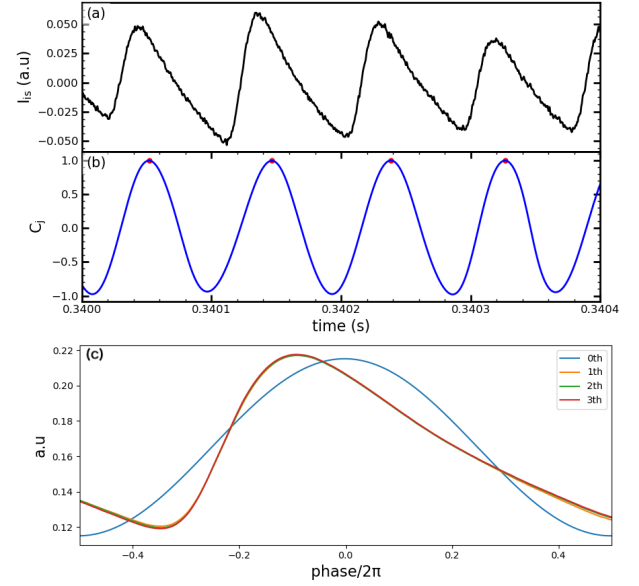


Fig. 2 Typical temporal evolution of ion saturation current at $r = 43$ mm (a) and trigger function (b). (c) initial template and templates after 1-3th iterations.

$$C_j(t) = \frac{1}{\sigma_F(t)\sigma_f} \int_{-T/2}^{T/2} (F(t' - t) - \bar{F}(t)) \cdot (f_j(t') - \bar{f}_j) dt' \quad (1)$$

Here j denotes number of iterations and $f_j(\tau)$ is the j -th template, $\bar{F}(t)$ and \bar{f}_j are averaged values of $F(t)$ and $f(t)$ over the fundamental period and $\sigma_F(t)$ and σ_f are variances of them. When pattern similar to the template is found in the original signal, $C_j(t)$ becomes large. Thus the $C_j(t)$ is used as an index of appearance of template in the original signal. Figure 2(b) shows the $C_0(t)$ calculated by the initial template. In the electrocardiogram analysis, template of heart-beat signal is already known. In plasma turbulence, however, the temporal pattern is generally not known. In our method, the pattern is determined self-consistently by a trial and error manner, and thus iteration process is required. We extracted sub-signals for each $100 \mu\text{s}$ from original signal based on peaks (local maxima) of $C_j(t)$ (see Fig. 2(b)) and averaged them again to obtain new template. We iterated above process until the template converges. Figure 2(c) shows templates obtained at different iteration loops (f_0 denotes the initial template). The template is converged after 3 iterations. More iterations are required in some cases [10].

We assume that high probability timing of appearance of the template is given by local maximum of the $C_j(t)$ and then the trigger function is given by a delta function ($\sum_i \delta(t - t_i)$, where t_i is the time-to-peak of $C_j(t)$). In that case, reconstructed waveform is written as $s(t) = \sum_i \{a_i \delta(t - t_i - \tau) f(\tau) + \bar{F}(t)\}$ by using the template, where $-T/2 \leq \tau \leq T/2$ and a_i is intensity of the template. The trigger function and reconstructed waveform are shown in Fig. 3.

The template is distorted from sinusoidal waveform

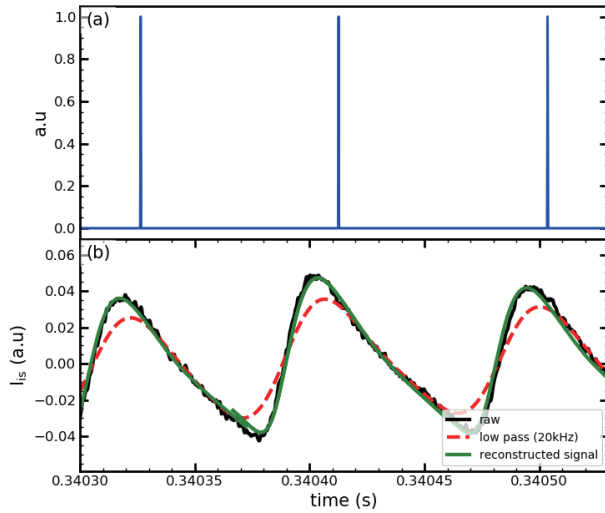


Fig. 3 (a) trigger function and (b) reconstructed signal. Original and low-pass-filtered (cut-off frequency is 30 kHz by using Bessel filter) signals are also shown.

and is similar to sawtooth wave which contains higher harmonics. In the case of extracting a coherent wave which has many higher harmonics, care should be taken when one applies digital filtering to signal. Strong filtering will break phase delay and group delay of higher harmonics. In our method, wave components which have regular phase delay with respect to the template are emphasized while those with random phase delay are canceled out through conditional averaging and thus this method realizes strong noise reduction without phase delay and group delay of higher harmonics.

3. Result and Discussion

Based on converged trigger function, we obtained statistical features of appearance frequency of the quasi-periodic 11 kHz fluctuation. The instantaneous periods of fluctuation are evaluated by the intervals between two adjacent peaks in the trigger function. The histogram of appearance frequency of the instantaneous period is shown in Fig. 4. This clearly demonstrates that the period of fluctuation in turbulent plasma varies in time and is distributed. The mean value and standard deviation of the distribution function are $8.73 \mu\text{s}$ and $3.98 \mu\text{s}$, respectively. These correspond to frequency of the fluctuation of 11 kHz. Kurtosis of them is 0.150 which is close to Gaussian, while skewness is found to be finite (0.335). Fluctuations in turbulent plasma are considered to be linearly excited and damped through nonlinear mechanisms. Thus, the appearance frequency and its statistical features (e.g. standard deviation) could be related to not only linear instability but also nonlinear dumping of fluctuations.

To compare the template method with the traditional conditional averaging method, we have applied the traditional reference time detection method used in blob analy-

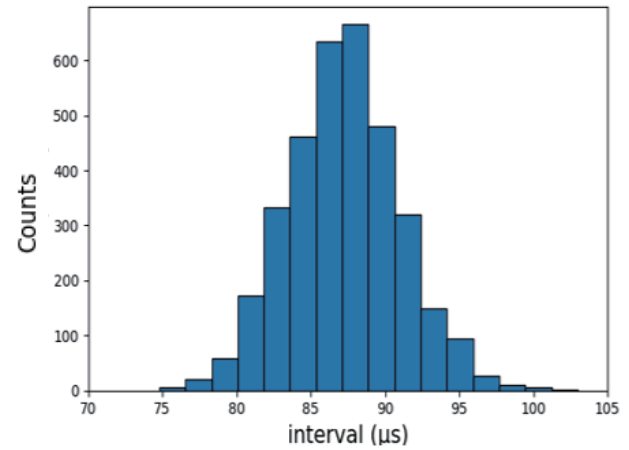


Fig. 4 Histogram of instantaneous intervals between peaks of trigger function.

sis [11], in which time-to-peak of pulse (t_i) is determined by $F(t_i) \geq F_{th} > F(t_{i-1})$, where time series signal $F(t_i)$ is sampled every $\delta t (t_i = t_{i-1} + \delta t)$ and F_{th} is a threshold value. Results are shown in Fig. 5. We have tested 2 threshold values which are indicated as blue and green broken lines in Fig. 5 (a). Determined time-to-peaks are shown as delta function in Fig. 5 (b) as blue and green lines corresponding to each threshold value. Trigger function determined by our method is also indicated (red line). There is a possibility of count error depending on the noise level and threshold value. An algorithm avoiding count error due to noise (e.g. smoothing) and suitable threshold value are required. They will be usually determined by a trial and error manner. Count error will cause doubling (or tripling) of the period. In fact, histogram of appearance frequency shows the doubling and tripling of period, while our method does not miss the counting as shown in Fig. 5 (c). In the case of pulse-like signals, e.g. blobs and ELMs, the traditional method is very powerful. While the template method is useful to determine a quasi-coherent wave-like pattern in a signal.

Based on the trigger function obtained at $r = 43 \text{ mm}$, templates at different radii. can be evaluated from signals of radial probe array. It is found that the 11 kHz fluctuation is large and localized in the narrow radial region (33 - 43 mm) as shown in Fig. 6 (a). Extracted templates have phase delay in the radial direction (Figs. 6 (b) - (f)). If we assume that $m = 4$ and rigid-body rotation, i.e. the templates at different radii propagate in the azimuthal direction together, we can draw equi-phase lines on azimuthal cross section, i.e. wave-front. Distorted waveforms of templates mean wave-fronts are twisted as shown in Fig. 7 (a). Obtained image is consistent with a result of visible light tomography [12, 13].

Waveform of the density fluctuation will be modified by Zonal flow/streamer and thus wave front distortion of density fluctuation ought to accompany with the distortion

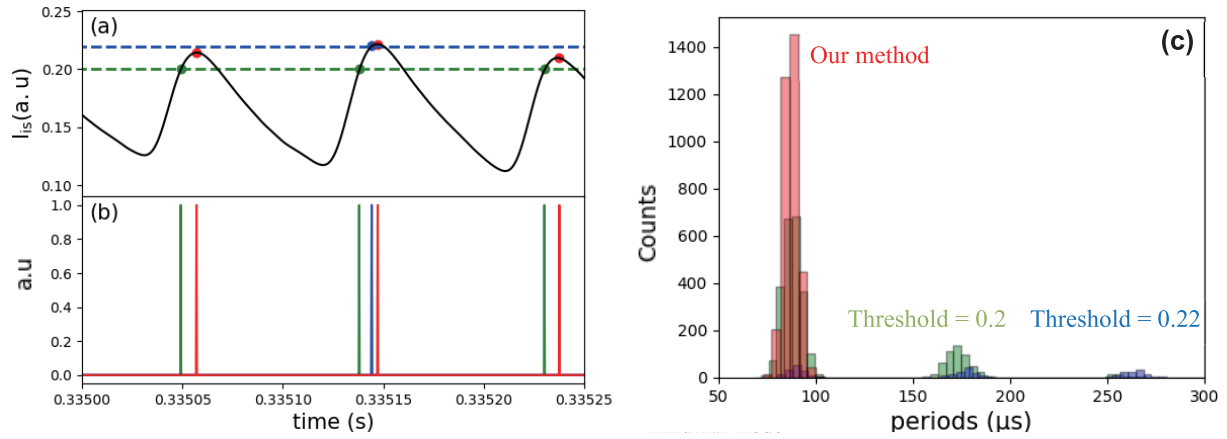


Fig. 5 (a) Example of reference time detection by the traditional method with 2 different thresholds of 0.2 (green) and 0.22 (blue). (b) Detected time-to-peak indicated by delta functions. (c) Appearance frequency of the fluctuation pattern with each method.

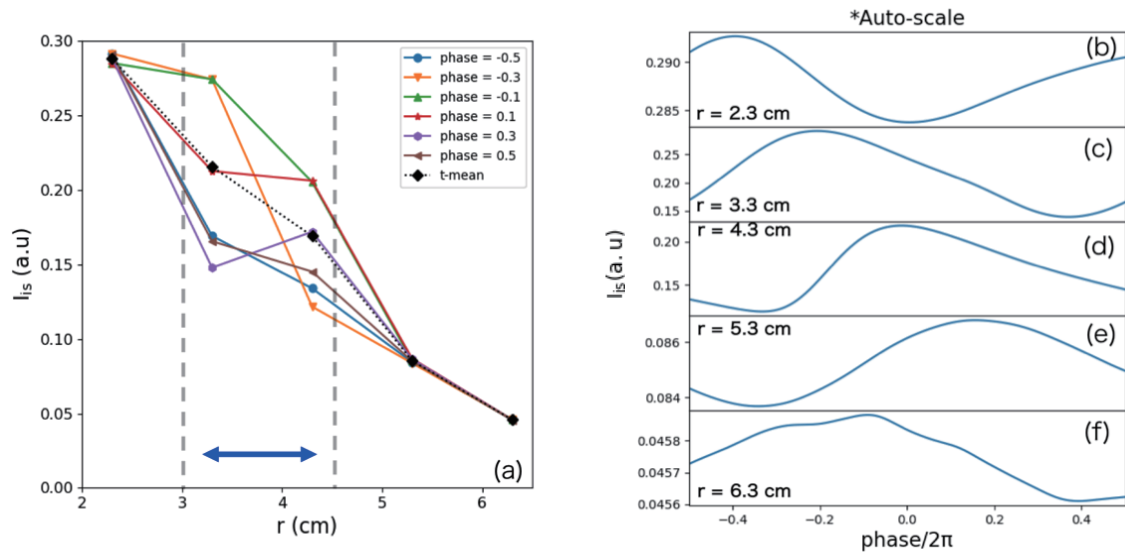


Fig. 6 Temporal change of radial profile of ion saturation current (a) and phase relation of templates at different radii. (b) - (f).

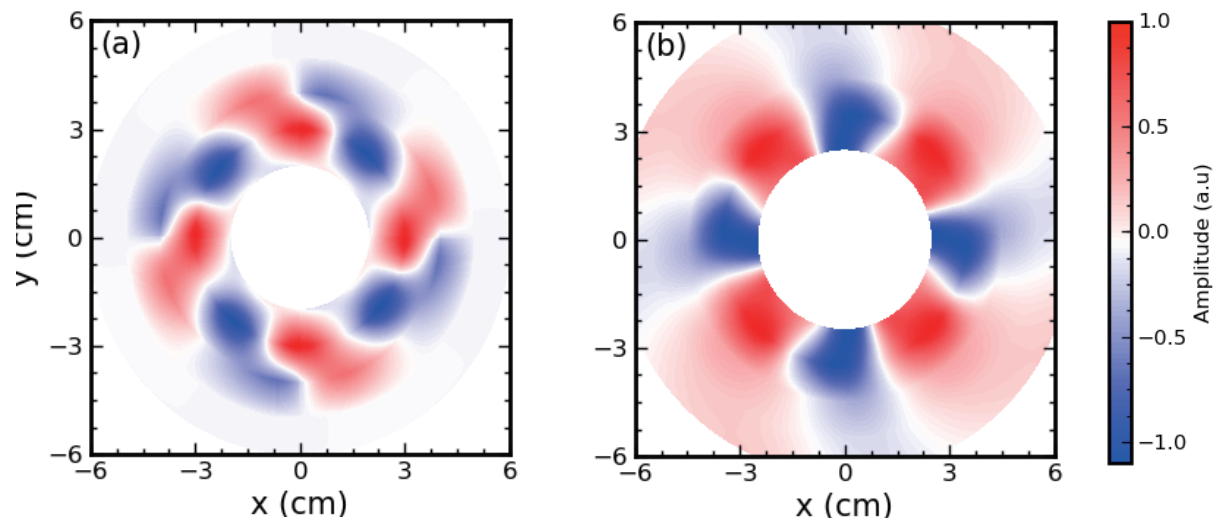


Fig. 7 Reconstructed density (a) and potential (b) fluctuation image on azimuthal cross section. Rigid-body rotation and $m = 4$ are assumed.

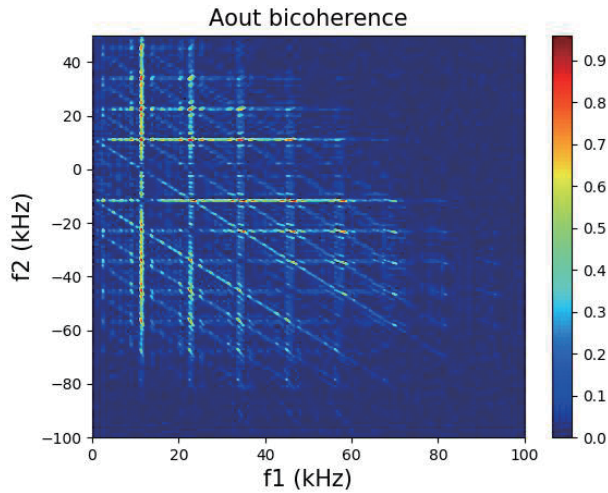


Fig. 8 Auto-bi-coherence of ion saturation current fluctuation at $r = 43$ mm.

of potential fluctuation. We reconstructed a 2-dimensional structure of potential fluctuation with almost the same experimental condition ($B = 0.13$ T, $P_{rf} = 6$ kW). Actually, we obtained distorted waveform of potential fluctuation as shown in Fig. 7 (b). Wave-front distortion is considered to be related to three-wave coupling [5]. In fact, the auto bi-coherence at $r = 43$ mm demonstrates the strong three-wave coupling involving with 11 kHz mode and its higher harmonics as shown in Fig. 8.

The trigger function is very useful to synchronize other diagnostics. For example, if timings of laser injection of Thomson scattering system are measured together with trigger function, conditional averaging can be performed, to evaluate the electron temperature component of the fluctuation synchronous with template. This experiment is in progress and will be reported in near future [14].

4. Summary

To observe the spatiotemporal pattern of newly ob-

served fluctuating structure in PANTA, we applied statistical averaging method and characterized the quasi-periodic fluctuation. Experimental observation indicates 1) instantaneous period of the fluctuation is distributed, 2) the fluctuation is radially localized and 3) wave-front of the fluctuation is inferred to be distorted. Observation of details of spatiotemporal structure is important for understanding of plasma turbulence physics. Pattern recognition method used here is found to be very powerful and thus will be applied to another pattern recognition problems.

Acknowledge

This work was partially supported by the Grant-in-Aid for Scientific Research of JSPS of Japan (JP18K03578, JP17H6089, JP15H02155, JP15H02335), the collaborative Research Program of Research Institute for Applied Mechanics, Kyushu University and of NIFS (NIFS13KOCT001).

- [1] H. Arakawa *et al.*, Sci. Rep. **6**, 33371 (2016).
- [2] P.H. Diamond, S.-I. Itoh and K. Itoh, Plasma Phys. Control. Fusion **47**, R35 (2005).
- [3] M. Rosenbluth and F. Hinton, Phys. Rev. Lett. **80**, 724 (1998).
- [4] S. Champeaux and P.H. Diamond, Phys. Lett. A **288**, 214 (2001).
- [5] T. Yamada *et al.*, Nature Phys. **4**, 721 (2008).
- [6] S. Inagaki *et al.*, Sci. Rep. **6**, 22189 (2016).
- [7] C. Theiler *et al.*, Phys. Plasmas **18**, 055901 (2011).
- [8] J.H. Shin *et al.*, Conf. Proc. IEEE Eng. Med. Biol. Soc. **2008**, 1144 (2008).
- [9] A.O. Leung *et al.*, Magn. Reson. Med. **60**, 709 (2008).
- [10] S. Inagaki *et al.*, Plasma Fusion Res. **9**, 1201016 (2014).
- [11] G. Fuchert *et al.*, Plasma Phys. Control. Fusion **55**, 125002 (2013).
- [12] A. Fujisawa *et al.*, Plasma Fusion Res. **10**, 1201080 (2015).
- [13] K. Yamasaki *et al.*, Rev. Sci. Instrum. **88**, 093507 (2017).
- [14] K. Tomita *et al.*, Plasma Fusion Res. **12**, 1401018 (2017).